Mathematics, measurement and experience of rotations around 3 axes

Ann-Marie Pendrill

National Resource Centre for Physics Education, Lund University, Box 118, SE 221 00 Lund, Sweden and

Department of Physics, University of Gothenburg, SE 412 96 Göteborg, Sweden

E-mail: `Ann-Marie.Pendrill@fysik.lu.se`

Abstract. This paper focuses on an amusement ride involving rotations around three axes, which offers a large-scale illustration for the study of dynamics in three dimensions. The forces on the rider can be measured with comoving accelerometers. As a first approximation, the different motions can be treated separately, but the combination of rotations is found to lead to a relatively large Coriolis effect. A mathematical description of the motion automatically combines all the different effects and offers a useful programming exercise.

This is an author-created, un-copyedited version of an article in European Journal of Physics 40 015003 (2019). IOP Publishing Ltd is not responsible for any errors or omissions in this version of the manuscript or any version derived from it. The Version of Record is available online at https://doi.org/10.1088/1361-6404/aaee22

1. Introduction

Motion in three dimensions is common in engineering applications. Describing three-dimensional motion including combinations of acceleration and rotation is a challenge where mathematics plays a central role. For several years, I had the privilege of running problem-solving classes for the mechanics courses in the spring for first-year engineering physics students, who used the textbooks by Meriam and Kraige [1]. For dynamics problems with rotations in three dimensions around several axes, intuition based on everyday experiences is of little help. As the course progressed, I observed how students, one by one, learned to trust the mathematics and displayed happy confidence when they were able to solve these challenging problems. As students struggled to visualise generalised 3D motion, including rotating arms, links, shafts, cranks and disks, I wished I had access to real-life concrete examples. The Star Shape ride Mechanica (figure 1), which opened at Liseberg in 2015 would have been an excellent example to follow the study of rotating pendulum rides, [2, 3].

Today's smartphones include 3D accelerometers and gyros, giving students easy ways to measure acceleration and rotation, using e.g. the app Physics Toolbox Roller Coaster [4, 5] or PhyPhox [6, 7]. The interpretation of the data offers good practice in identifying coordinate axes [2, 3, 8].

Figure 1. The Star Shape ride Mechanica at Liseberg. When the ride is in motion the 12 m main arm rotates a full turn in 8 s around the X axis. At the same time the star, with a radius of 4 m, rotates a full turn in 10 s around the main arm. Each of the gondolas in the star seats 5 guests, and can rotate freely around its axis.

2. The Star Shape Ride Mechanica - combining rotations around three axes

Figure 1 shows the Star Shape ride from Zierer [9], which features rotations around three axes. After a few smaller oscillations the star reaches the top. The ride then continues with three full turns, each taking about $T = 8$ s, moving the center of the star in a large circle with radius $R = 12$ m around a horizontal axis (X), while the star rotates slowly ($T_{star} \approx 10$ s per turn) around the main arm. The motion stops for a while in the highest point, where the star changes its direction of motion. The main arm then makes a few full turns in the other direction. The gondolas of each arm can swing freely throughout the ride. Describing the changing location of one of the riders while the main arm makes full turns is a suitable programming exercise.

In addition to a mathematical description of the motion in a fixed coordinate system, we also need to consider the force from the ride on the rider, given by $m(\mathbf{a} - \mathbf{g})$,

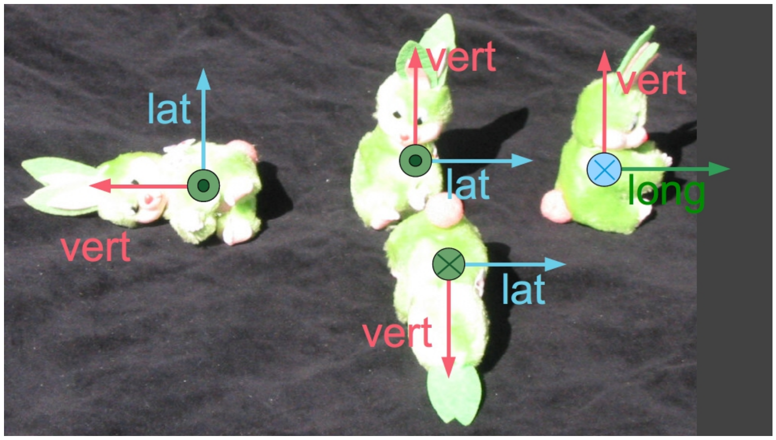

Figure 2. The comoving coordinate system used to describe biomechanical effect on riders. The vertical coordinate points along the spine towards the head. The longitudinal coordinate points in the forward direction and the lateral coordinate to the left.

since it needs to compensate for gravity, while also providing the force required for the acceleration. Biomechanical effects are traditionally expressed in a body-fixed coordinate system, which follows the rotation of the body, as shown in figure 2. In this rider-based coordinate system, "vertical" denotes the direction along the spine towards the head, "longitudinal" is in the forward direction and the "lateral" direction points to the left. Limits for the biomechanical forces in different directions were discussed in earlier work (e.g. [10]). These co-moving coordinates are also used for data from electronic accelerometers taken along on a ride.

Figure 3 shows accelerometer data collected during a ride in one of the seats furthest away from the centre of the star using a Wireless Dynamic Sensor System (WDSS) [11].

3. Mathematical description of the motion

3.1. The main rotation

The location $\mathbf{R}$ of the centre of the star can be defined in the stationary coordinate system, where the Z axis is vertical and the rotation of the main arm is around the X-axis, as shown in figure 1. A first step is to consider the main rotation, introducing an angular velocity Ω (figure 4), treated as constant when the ride is in motion.

We also introduce an angle $\theta = \Omega t$ to describe the orientation of the main arm at time t (figure 5). If we define the angle θ to be zero when the star is in the lowest position the coordinates of the centre of the star are given by

$$R_X = 0$$
$$R_Y = R\sin\theta$$
$$R_Z = -R\cos\theta$$

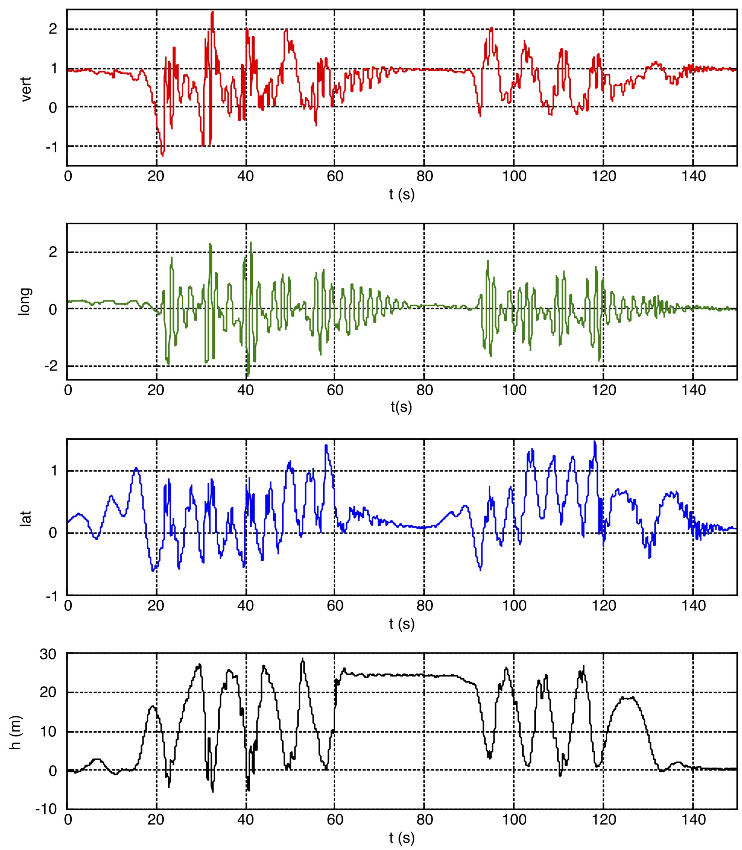

Figure 3. Accelerometer data for a rider in one of the outer seats of the Star Shape ride Mechanica collected with the WDSS sensor system [11]. The sensor was carried in a vest on the body. The data shows the components of the vector $(\mathbf{a}-\mathbf{g})/|g|$ for the three axes in the coordinate system of the rider, defined in figure 2. The final graph shows the elevation obtained from the WDSS (which converts the change in air pressure to an approximate value for elevation, leading to a lack of precision when the ride is in motion).

The location of the centre of the star can then be written in a number of representations, e.g. $\mathbf{R} = R_X\mathbf{i} + R_Y\mathbf{j} + R_Z\mathbf{k} = (R_X, R_Y, R_Z) = R(0, \sin\theta, -\cos\theta)$, where $\mathbf{i}$, $\mathbf{j}$ and $\mathbf{k}$ are the unit vectors in the fixed coordinate system defined in figure 1. We may also introduce a unit vector $e_R = (0, \sin\theta, -\cos\theta)$ pointing in the direction of $\mathbf{R}$.

For a period $T = 8\,\mathrm{s}$, the angular velocity is $\Omega = 2\pi/T \approx 0.79\,\mathrm{rad/s}$. The velocity, $\mathbf{v}_c$, and acceleration, $\mathbf{a}_c$, of the centre of the star can be written as

$$\begin{aligned} \mathbf{v}_c &= \quad R\Omega(0, \cos\theta, \sin\theta) \\ \mathbf{a}_c &= -R\Omega^2(0, \sin\theta, -\cos\theta) = -\Omega^2\mathbf{R} = -R\Omega^2 e_R. \end{aligned}$$

giving a speed $v_c = R\Omega \approx 9\,\mathrm{m/s}$ for $R = 12\,\mathrm{m}$ and a centripetal acceleration with the size $a_c = R\Omega^2 \approx 0.75g$.

Figure 4 illustrates the centripetal acceleration due to the main rotation. For riders close to the centre of the star, the description above gives a relatively good

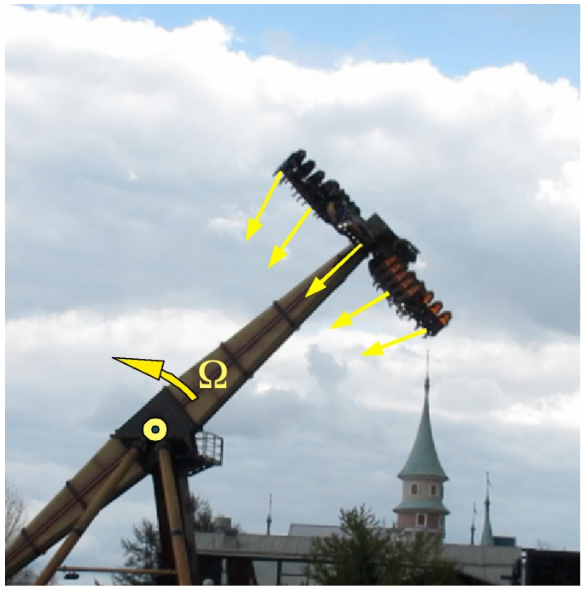

Figure 4. The Star shape ride viewed from the side. The arrows mark the centripetal acceleration due to the main rotation $\mathbf{\Omega}$, for a few different rider positions.

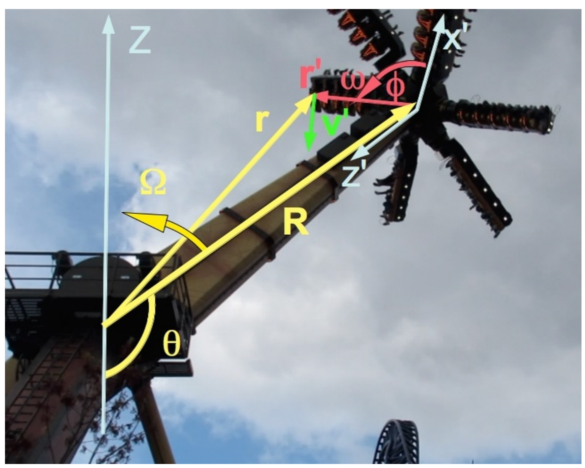

Figure 5. The location $\mathbf{r}$ of a rider is expressed as a sum of the vector $\mathbf{R}$ which gives the position of the centre of the star, and the vector $\mathbf{r}'$ which gives the position of the rider relative to the centre of the star. The main arm $\mathbf{R}$ rotates around the X axis with an angular velocity Ω, while the star rotates with an angular velocity ω around the main arm.

approximation. Below, we consider additional effects arising due to the rotation of the star, where the rider can be seated up to 4 m from the center.

3.2. Motion within the plane of the star

Figure 5 shows how the location $\mathbf{r}$ of a rider can be written as

$$\mathbf{r} = \mathbf{R} + \mathbf{r}'$$

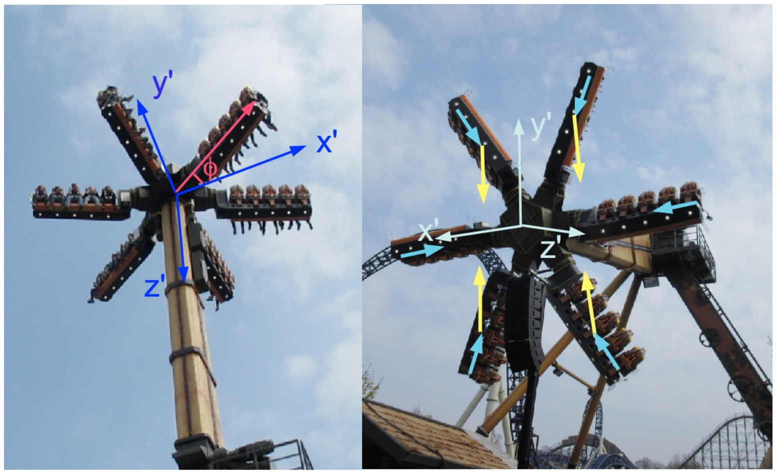

Figure 6. Coordinate system and centripetal accelerations in the plane of the star. The rotation of the star leads to an acceleration towards the centre of the star (shown in light blue arrows), of about $0.16\,g$ for a rider at the maximum distance. The main rotation is around the X axis, which coincides with the x' axis, and only causes centripetal acceleration components orthogonal to that axis. The component of the centripetal acceleration in the plane of the star due to the main rotation is $d\Omega^2 \sin\phi \approx 0.25\,g \sin\phi$ and is shown by (yellow) arrows pointing up or down in the figure to the right (i.e along the y' axis).

where the vector $\mathbf{R}$ gives the position of the centre of the star as discussed above, and the vector $\mathbf{r}'$ which gives the position of the rider relative to the centre of the star:

$$\mathbf{r}' = x'e'_x + y'e'_y + z'e'_z. \tag{1}$$

The axes of the coordinate system of plane of the star are chosen so that the z' axis points towards the center of the ride along the main arm and the x' and X axes coincide (figures 6 and 7). Thus the direction of the x' axis does not change during the motion.

The position of the rider within the plane of the star can be expressed in terms of a distance, $d \leq 4m$, from the centre of the star and an angle, ϕ, which changes as the star rotates.

$$x' = d\cos\phi$$
$$y' = d\sin\phi$$
$$z' = 0$$

The location, $\mathbf{r}'$, within the plane of the star can also be expressed in terms of polar coordinates as

$$\mathbf{r}' = d(\cos\phi\, e'_x + \sin\phi\, e'_y) = de'_r \tag{2}$$

If the star rotates the with an angular velocity ω, the angle ϕ can be written as $\phi = \phi_0 + \omega t$. If the star makes a full turn in $T_{star} = 10\,\mathrm{s}$, the corresponding angular velocity is given by $\omega = 2\pi/T_{star} \approx 0.63\mathrm{rad/s}$.

The velocity within the plane of the star can be written

$$\mathbf{v}' = v'(-\sin\phi e'_x + \cos\phi e'_y) = v'e'_\phi \tag{3}$$

where the speed is given by $v' = d\omega$. Similarly, the acceleration due to the rotation of the star can be written as

$$\mathbf{a}'_c = -\mathbf{r}'\omega^2 = -d\omega^2 e'_r = -d\omega^2(\cos\phi\, e'_x + \sin\phi\, e'_y). \tag{4}$$

For riders seated in the outer part of a gondola, $a'_c \approx 0.16\, g$.

Figure 6 illustrates this centripetal acceleration, together with the components in the plane of the star of the centripetal acceleration due to the main rotation, which can reach $d\Omega^2 \approx 0.25g$.

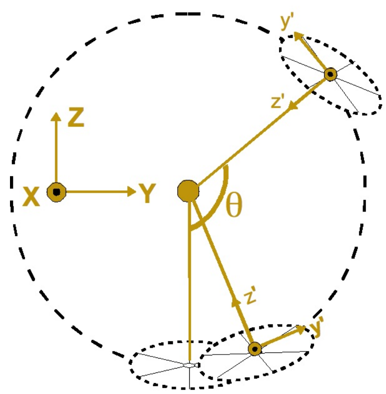

Figure 7. Rotation of the coordinate system of the star.

3.3. Rotating coordinate axes

The main rotation leads to a rotation of the plane of the star. The coordinate system $x'y'z'$ can be expressed in terms of fixed coordinate system as

$$\begin{aligned} e'_x &= \mathbf{i} \\ e'_y &= \cos\theta\,\mathbf{j} + \sin\theta\,\mathbf{k} \\ e'_z &= -\sin\theta\,\mathbf{j} + \cos\theta\,\mathbf{k} \end{aligned}$$

The position of the rider within the plane of the star can be written in terms of comoving coordinate axes e'_r and e'_ϕ, where e'_r points out from the center of the star towards the rider and e'_ϕ points in the direction of motion, as introduced in the equations (2) and (3).

$$e'_r = \cos\phi\,\mathbf{i} + \sin\phi\cos\theta\,\mathbf{j} + \sin\phi\sin\theta\,\mathbf{k} \tag{5}$$

$$e'_\phi = -\sin\phi\,\mathbf{i} + \cos\phi\cos\theta\,\mathbf{j} + \cos\phi\sin\theta\,\mathbf{k} \tag{6}$$

Using these coordinate axes, the location of a rider in the star, $\mathbf{r} = \mathbf{r}' + \mathbf{R}$, can be expressed in the fixed coordinate system, giving

$$x_s = d\cos\phi \tag{7}$$

$$y_s = d\sin\phi\cos\theta + R\sin\theta \tag{8}$$

$$z_s = d\sin\phi\sin\theta - R\cos\theta \tag{9}$$

3.4. Velocity and acceleration in the combined motion

Assuming constant angular velocities, the angles can be written as $\theta = \Omega t$ and $\phi = \omega t + \phi_0$. Taking the time derivative of the expressions in (7)-(9) then gives the components of the velocity

$$\begin{aligned} v_x &= -d\,\omega \sin\phi \\ v_y &= d(\omega\cos\phi\cos\theta - \Omega\sin\phi\sin\theta) + R\Omega\cos\theta \\ v_z &= d(\omega\cos\phi\sin\theta + \Omega\sin\phi\cos\theta) + R\Omega\sin\theta. \end{aligned}$$

Similarly, the time derivative of the velocity components gives expressions for the acceleration

$$\begin{aligned} a_x &= -d\,\omega^2\cos\phi = -x\omega^2 \\ a_y &= d(-\omega^2\sin\phi\cos\theta - \Omega^2\sin\phi\cos\theta - 2\omega\Omega\cos\phi\sin\theta) - R\Omega^2\sin\theta \\ a_z &= d(-\omega^2\sin\phi\sin\theta - \Omega^2\sin\phi\sin\theta + 2\omega\Omega\cos\phi\cos\theta) + R\Omega^2\cos\theta. \end{aligned}$$

The acceleration vector can also be expressed as

$$\mathbf{a} = -\mathbf{R}\Omega^2 - \mathbf{r}'\omega^2 + 2\mathbf{\Omega}\times\mathbf{v}'. \tag{10}$$

The additional term is the Coriolis effect, which appears for motion within a rotating coordinate system and is ortogonal to the rotation axis and to the relative velocity. Inserting numerical values shows that this case, the Coriolis effect can contribute up to $0.40g$ in the positive or negative z' direction.

Figure 8. The motion of a rider passing the lowest point of the ride, while the star rotates around the main arm and the gondola swings back and forth. The arrows mark the "up" direction for the rider, corresponding to the "vertical" axis in figure 2. (The time interval between the screen shots is 0.4 s.)

3.5. Freely rotating gondola

The final rotation involves the gondolas which can rotate freely around the arm of the star. Figure 8 shows an example of their motion as the ride passes the lowest point.

As the ride stops at the top, the gondola continue to swing back and forth in damped oscillations around the equilibrium orientation, as can be seen from the vertical and longitudinal data in figure 3 (at about $60s - 75$ s in the graph).

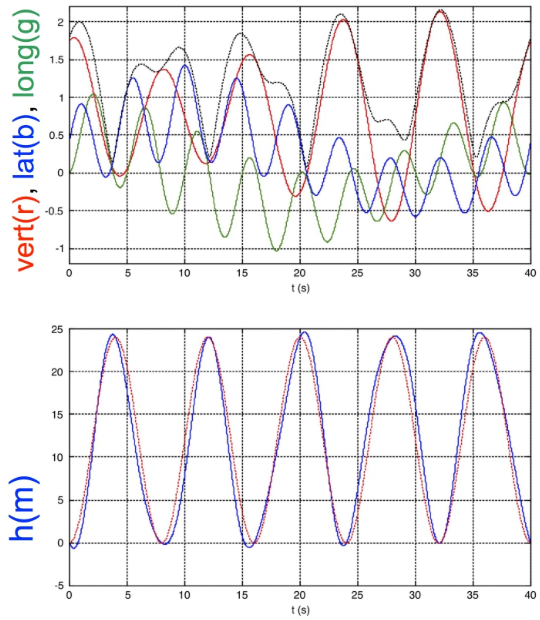

Figure 9. Calculated values for the different components of the g factor. The first graph shows the calculated vertical, lateral, and longitudinal components, as well as size of the total g factor (dotted). (In the calculations, the rotation of the gondola is omitted, and "vertical" direction corresponds to the z' axis and the longitudinal to the direction of motion given by e'_ϕ.) The second graph shows the elevation of the center of the star (dotted), given by $R\cos\theta$, and of a rider at maximum distance from the center of the rotating star (solid).

3.6. Forces on the rider

The total force on the rider can be expressed as $m\mathbf{g} + \mathbf{X} = m\mathbf{a}$ where $\mathbf{X} = m(\mathbf{a} - \mathbf{g})$ is the force from the ride in the fixed coordinate system. It is related to the components of the acceleration as

$$X_x/m = a_x$$
$$X_y/m = a_y$$
$$X_z/m = g + a_z$$

where $g = |\mathbf{g}| \approx 9.82\text{m}/s^2$. The "G force" or "g factor" can be defined as a normalized force vector $\mathbf{G} = \mathbf{X}/mg = (\mathbf{a} - \mathbf{g})/g$, which is independent of the mass of the rider. For the rider, it is more interesting to know the forces in the coordinate system moving together with the rider, which would also be the forces measured by a comoving accelerometer.The lateral component is defined by the direction e'_r in (6) as $X_{lat} = -\mathbf{X} \cdot e_r{}'$.

If we neglect the rotation of the gondola itself, the coordinate in the direction of the motion within the star, $\mathbf{v}'$, corresponds to the "longitudinal" component, i.e. $X_{long} = \mathbf{X} \cdot e'_\phi$. Finally, the "vertical" component is along the z' axis, i.e. $X_{vert} = \mathbf{X} \cdot e'_z$.

Figure 9 shows the result of the theoretical model with a rider at the maximum distance, 4m, from the center in a gondola starting with a phase $\phi = -90^o$ at $t = 0$, which can be compared to the experimental data in figure 3.

4. Challenging comparisons

Comparing amusement ride accelerometer data to calculated values can be challenging on many levels. The manufacturer www site [9] only specifies number of riders, capacity and outer dimensions which are not sufficient for physics assignments. Some data may be obtained by measurements on-site, but more direct contact with the park can give more precise dimensions. Due to safety considerations, prior arrangement should be also made with the park before a sensor is brought on a ride. The axis orientation precision is limited in how well the sensor is attached to the body of the rider - and rider motion within the seat may change the orientation.

The data collected are often noisy, as seen from the graphs. Vibrations in the ride, but often also small oscillations from the sensor itself contribute to the noise.

In the case of the Star Shape ride, the free rotation of the gondola includes an element of motion which is not pre-determined. This complicates the comparison between calculated and measured values. However, it is possible to compare g factors for a few situations discussed below.

4.1. Gondola oscillations

The main rotation stops for a while in the highest point, offering a view of the gondola oscillations, without the added complication of the changed direction of the gravitational field relative to the gondola. Figure 10 shows details of the vertical and longitudinal g factors during the oscillations at the top, as well as when the star passes the lowest points. The period of oscillation is $T_g \approx 2\,\mathrm{s}$ at the top, as seen from the graph in figure 10. This corresponds to a radius of gyration $r_g \approx 1\,\mathrm{m}$, which is the length of a mathematical pendulum with the same period.

If α denotes the maximum angle between the acceleration of gravity and the vertical axis of the rider the g factor in this "vertical" direction varies between $\cos\alpha$ and $(1 + 2(1 - \cos\alpha))$ for a sensor placed at the distance r_g, whereas the longitudinal g factor vanishes, (see e.g. [3, 12]). However, the data shown in figures 3 and 10 were collected with the sensor worn in a vest close to the "heartline", which is also close to the axis for the gondola oscillations, as seen e.g. from the movie and photos at the Zierer Star Shape www site [9]. For this case, the vertical g factor is instead expected to vary between $\cos\alpha$ and 1, whereas the longitudinal g factor varies between $\sin\alpha$ and $-\sin\alpha$, changing sign during the swinging to and fro. The longitudinal component of the g factor gives the clearest indication of the gondola oscillations.

As the star passes the lowest point while the main arm rotates, the g factors related to the oscillations of the gondola are increased by a factor of 1.75, due to the acceleration of centre of the star (about $0.75g$) which increases the apparent gravitational field,

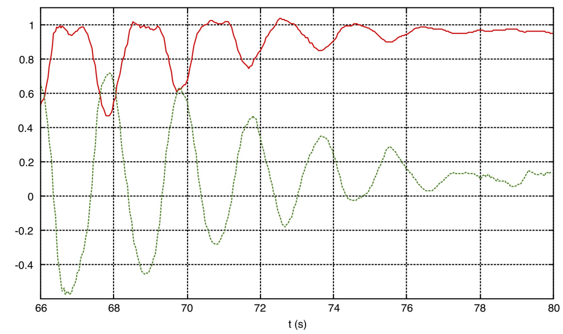

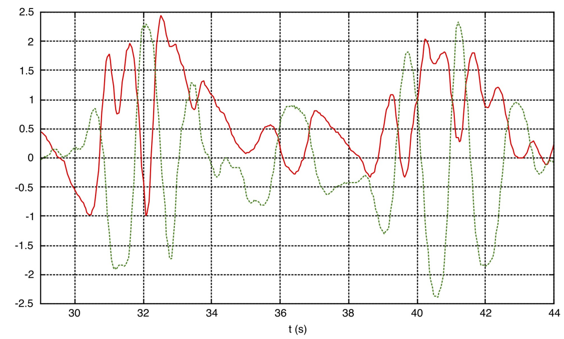

Figure 10. Vertical (red, solid) and longitudinal (green, dotted) g factors showing the oscillations of gondola. The upper graph shows the oscillations as the star is in the highest position, whereas the lower graph shows the oscillations as the star passes the lowest point twice. The asymmetry in the vertical g factor arises from the sensor leaning slightly backwards when carried on the author's body.

$(\mathbf{g}-\mathbf{a})$. This is also expected to lead to a reduction of the oscillation period by a factor of $\sqrt{1+0.75}$, giving an expected gondola oscillation period of 1.5 s in the lower part, essentially confirmed by the data (figure 10). Also, the series of screen shots in figure 8 show that a half-period is slightly shorter than 0.8 s.

4.2. Lateral forces and the rotation of the star

Since the lateral force is not affected by the gondola oscillations, this comparison is more direct than for the other components. The rotation of the star making a full turn in 10 seconds leads to a centripetal acceleration, towards the centre of the star, which points to the left of the rider, making a positive contribution of 0.16 to the lateral g factor ($d\omega^2 \approx 0.16\,g$). Depending on the position in the star, the main rotation can give an additional positive contribution of up to 0.25, as shown in figure 6. When the star passes the highest or lowest positions, the star is in a horizontal plane we expect lateral (sideways) forces from the ride in the range $0.16g$ to $0.41\,g$.

Between the highest and lowest points, the star is, instead, in a completely vertical plane (figure 6). The lateral force from the ride then also needs to compensate for the the part of gravity that is not used for acceleration. For a rider in highest part of the star, the force required from the ride is $mg(1 - 0.16 - 0.25) = 0.59mg$, upward, and out from the centre of the star. This points to the right of the rider, giving a negative lateral g factor of -0.59.

In the lowest part of the star, the force from the ride is still upwards, but to the centre of the star and to the left of the rider. The force must compensate for gravity and also supply the force for the acceleration of $0.41g$. The sideways force needed from the ride is then $1.41mg$, pointing to the left of the rider, giving a lateral g factor of 1.41.

Both the theoretical and measured lateral g factors, in figures 9 and 3, fall between -0.59 and 1.41 throughout the ride.

4.3. Vertical and longitudinal forces in the highest and lowest points

A 12 m long arm rotating uniformly at with a period of 8 s would lead to a centripetal acceleration of $0.75g$ at the centre of the star. As the star passes the lowest point, an upward force of $mg(1 + 0.75)$ from the ride is needed to provide this acceleration for a rider. However, depending on the position in the rotating star, the Coriolis effect implies an upward or downward acceleration of up to $0.40g$. We would thus expect a maximum upward force on the rider of $(1.75 + 0.40)\,mg = 2.15\,mg$, and a minimum force of $1.35\,mg$ or a vertical g factor in the highest point to be between 1.35 and 2.15.

In the highest point an upward force from the rid of $0.25\,mg$ added to the force of gravity would allow for a downward acceleration of $0.75\,g$. The Coriolis effect can change the required force to values between $0.65\,mg$ upward and $0.15\,mg$ downwards. In the calculations, the rider is assumed to be oriented with the head pointing down, which inverts the sign for the vertical g factor, which is then expected to be between -0.65 and $+0.15$, which agrees well with the theoretical values in figure 9.

Due to the rotation of the gondola, this "vertical" component of the g factor will be distributed over the vertical and longitudinal components in the measured data. In figure 10, we note how the maximum values of the longitudinal g factor is comparable to the maximum values for the vertical g factor.

The maximum total g factor is slightly larger than the values 2.15 expected from the calculations, as seen from the graphs in figures 3 and in more detail in figure 10. This discrepancy can be understood by noting the that the rotation of the main arm is slightly faster when the star is in the lower half of the rotation. This can be seen from a video of the movie, but also from the measured elevation data.

4.4. Longitudinal forces for the star in a vertical plane

In the theoretical calculations, the longitudinal direction coincides with the e'_ϕ axis in the plane of the star. Intuitively, we might expect the longitudinal force on the rider to be $mg\cos\phi$ when the star is in a vertical plane, with the largest values, $\pm mg$, in situations where the rider sits in a gondola aligned with the horizontal x' axis. However, the calculated graphs in figure 9 show values slightly outside these expected limits. Mathematics can beat intuition!

To understand the small deviations, we need to consider the centripetal acceleration due to the main rotation, illustrated in figure 6. If the rider is located at an angle ϕ from the horizontal axis, the contribution to the lateral g factor is $-d\Omega^2 \sin\phi \sin\phi/g$ and to the longitudinal component $-d\Omega^2 \sin\phi \cos\phi/g$. The total longitudinal g factor is then $\cos\phi(1 - d\Omega^2 \sin\phi/g)$, which can be slightly larger than 1 for small negative angles ϕ. Similarly, for angles just over 180^o, the longitudinal g factor can have a slightly more negative value than -1.

5. Discussion

Intuition often fails in the study of forces in three dimensional motion involving rotation. In this paper, we have considered forces on a rider, by adding contributions resulting from the different centripetal accelerations, as well as the Coriolis effect. The values are first compared with theoretical results, where the effect of the rotating gondola has been neglected. The mathematical description automatically includes complex combinations of the different contributions to the force from the ride on the rider.

Comparisons between theoretical and experimental values are complicated by the pendulum motion of the gondola. Since the sensor is placed close to the gondola axis, additional forces can be neglected, but the rotation of the gondola leads to a mixing of vertical and longitudinal components of force on the rider, and only maximum values can be compared directly. The measured data show that forces in the lowest point can reach higher values than expected. These can be accounted for by noting that the rotation is faster when the star is closer to the ground, as revealed by elevation data in figure 3. The uneven rotation can also be seen in the accompanying video abstract.

The example of the Star Shape ride shows how data from the ride can be compared with theoretical expectations at different degrees of complexity. During introductory courses, looking into one motion at a time, will be sufficiently challenging. Many other rides offer more easily accessible modelling examples, such as roller coaster loops [13, 14, 15] and brakes [17]. Amusement park visits also offer a wide range of other activities that support conceptual understanding in physics and engineering education [18, 19, 20, 21, 22].

When students have learned to work with rotations in three dimensions and encountered transformations between different coordinate systems, writing a program small program to model the position in the Star Shape ride, as well as the forces on the rider, gives useful practice. The ride considered in this paper offers an illustration of the power of mathematics to include the different contributions, without having to consider explicitly the vector addition of the different force contributions.

Acknowledgments

I would like to express my appreciation to the Liseberg amusement park for support, both in the form of ride tickets for engineering students and technical data for the rides, as well as data collection opportunities. I would also like thank students who have participated in amusement park projects, often bringing enthusiasm to the projects with work far surpassing course requirements.

References

[1] Meriam J L and Kraige L G 2008 *Engineering Mechanics: Dynamics*, 6th edition, Wiley

[2] Pendrill A-M and Rohlén J 2011 Acceleration and rotation in a pendulum ride, measured using an iPhone 4 *Physics Education* 46 676-681 doi.org/10.1088/0031-9120/46/6/001

[3] Pendrill A-M and Modig C 2018 Pendulum rides, rotation and the Coriolis effect *Physics Education* 53 4 045017 doi.org/10.1088/1361-6552/aac3cb

[4] Vieyra C 2016 *Physics Toolbox Roller Coaster* vieyrasoftware.net/

[5] Vieyra R and Vieyra C Analyzing Forces on Amusement Park Rides with Mobile Devices *The Physics Teacher* 52, 149, doi.org/10.1119/1.4865516

[6] *Physics Phone Experiments, PhyPhoX* phyphox.org

[7] Staacks S, Hütz S, Heinke H and Stampfer C 2018 Advanced tools for smartphone-based experiments: phyphox *Physics Education* 53 045009, doi.org/10.1088/1361-6552/aac05e

[8] Löfström M and Pendrill A-M 2016 Aerodynamics in the amusement park: interpreting sensor data for acceleration and rotation *Physics Education* 50 055015 doi.org/10.1088/0031-9120/51/5/055015

[9] Zierer Karussell und Spezialmaschinenbau GmbH *Star Shape* http://www.zierer.com/en/products/major-rides/star-shape.html, including a video https://www.youtube.com/watch?v=YFDM0ns1R4Y

[10] Eager D, Pendrill A-M and Reistad N 2016 Beyond velocity and acceleration: jerk, snap and higher derivatives *European Journal of Physics* 37 6 065008 doi.org/10.1088/0143-0807/37/6/065008

[11] Vernier 2018 *Wireless Dynamic Sensor System* www.vernier.com/products/sensors/wdss/

[12] Tornara F, Monteiro M and Marti A C 2014 Understanding coffee spills using a smartphone *The Physics Teacher* 52 502

[13] Pendrill A-M 2005a Roller coaster loop shapes *Physics Education* 40 517 doi.org/10.1088/0031-9120/40/6/001

[14] Nordmark A B and Essén H 2010 The comfortable roller coaster - on the shape of tracks with a constant normal force *European Journal of Physics* 31 1307 doi.org/10.1088/0143-0807/31/6/001

[15] Pendrill A-M 2013 Student investigations of forces in a roller coaster loop *European Journal of Physics* 34 1379 doi.org/10.1088/0143-0807/34/6/1379

[16] Alberghi S, Resta L and Gaudenzi S 2013 Experiencing mathematical modelling in an amusement park *Journal of Mathematical Modelling and Application* 1 3

[17] Pendrill A-M, Karlsteen M and Rödjegård H 2012 Stopping a roller coaster train, *Physics Education* 47 728-735 doi.org/10.1088/0031-9120/47/6/728

[18] Bakken C 2018 *Physics, Science & Math Days @ California's Great America*, physicsday.org

[19] Pendrill A-M and Rödjegård H 2005 *A roller coaster viewed through motion tracker data Physics Education* 40 522-526 doi.org/10.1088/0031-9120/40/6/002

[20] Pendrill A-M 2016 Rotating swings - a theme with variations *Physics Education* 51 15014 doi.org/10.1088/0031-9120/51/1/015014

[21] Bagge S and Pendrill A-M 2002 Classical physics experiments in the amusement park *Physics Education* 37 507-511

[22] Pendrill A-M 2008 How do we know that the Earth spins around its axis? *Physics Education* 43 158-164